

Melt Blending of Linear Low-Density Polyethylene and Polystyrene in a Haake Internal Mixer. II. Morphology-Processing Relationships

LI-YING YANG,¹ DAVID BIGIO,² and THEODORE G. SMITH^{1,*}

¹Department of Chemical Engineering and ²Department of Mechanical Engineering, University of Maryland, College Park, Maryland 20742

SYNOPSIS

A measure of the effective shear rate range for dispersive mixing in the Haake mixer has been developed, which is more representative of shearing conditions than that currently used. In addition, the effects of processing conditions, composition, and compatibilizer on linear low-density polyethylene and polystyrene (LLDPE/PS) blend morphology were studied. Fiber/stratified morphologies form with blends when the minor phase has low viscosity and is present at its higher concentration. The influence of the viscosity ratio on phase size was found to be a minor effect for mixtures having a low fraction of the dispersed phase (20% PS). The effect of shear intensity, however, was found to be more important at a low composition of the dispersed phase or in compatibilized blends. During Haake blending, an optimal time for adding compatibilizer to stabilize phase morphology was found to be when the final morphology of an incompatible blend had developed. Further studies have concluded that the addition of styrene-ethylene/butylene-styrene (SEBS) stabilized the blend morphology of LLDPE/PS more efficiently than styrene-ethylene/propylene (SEP) on different blending conditions and compositions. At high temperatures, the addition of SEP to a LLDPE/PS blend did not modify the dispersed phase size. On the other hand, SEBS stabilized the dispersion so that the final domain size is independent of composition. © 1995 John Wiley & Sons, Inc.

INTRODUCTION

The phase morphology generated during melt processing has a significant influence on the performance of blends. The interrelationship between processing morphology and the final physical and mechanical properties of polymer blends has been gaining considerable attention.¹ The size and shape of the minor phase, for example, are critical to the impact properties.^{2,3} The processing parameters (mixing history and the effect of heat treatment),⁴⁻⁶ material characteristics (rheological properties and compatibility),⁷⁻⁹ and composition^{10,11} are the most important factors in determining the final droplet size and shape during polymer blending.

A Haake internal mixer (i.e., the measuring head of the Brabender Plasti-Corder torque rheometer) not only functions as a small scale of the Banbury mixers in industry but also serves as a viscometer. The irregular-shaped roller blades induce a very complex flow field in the mixing chamber (see Fig. 1), which makes rheological interpretation of Haake mixer data difficult. Previous studies have converted torque-rheometer data into approximately equivalent units of viscosity and shear rate using correlations based on instrument dimensions.¹²⁻¹⁴ Goodrich and Porter¹² simulated the Haake as two uniform concentric-cylinder, constant-speed rotational viscometers which require the same torque as the irregularly shaped roller blades. By calibration with a Newtonian liquid, the effective diameter of the inner cylinders can be calculated. The Haake blender is driven from a common shaft but geared so the roller speeds have a ratio of 3 to 2. At a rotor speed N , the shear rate in the Haake mixer was then cal-

* To whom correspondence should be addressed.

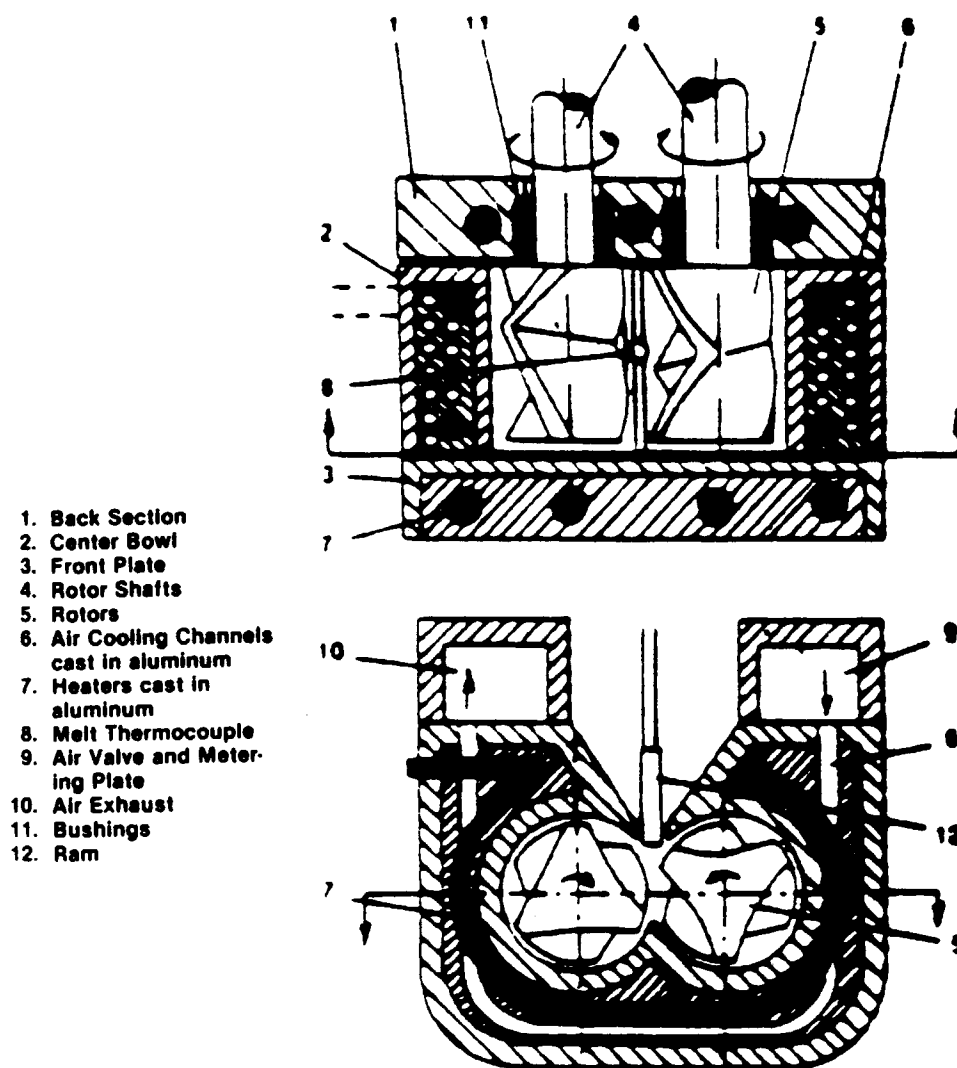


Figure 1 Schematic of the Haake blender.³²

culated as $0.76N$ and $1.14N$ for the low- and high-speed rollers, respectively. When considering non-Newtonian materials, and the influence of different rotation speeds on the average shear between two adjacent (not-well separated) coaxial cylinders, Lee and Purdon¹⁴ found an unexpected variation of the shear rate in the Haake mixer with different polymers. Recently, Serpe et al.⁴ compared the viscosities of blends of polyethylene (PE) and polyamide (PA), measured during mixing in the Haake instrument (by torque-rpm relationship), with the melt rheology determined with a capillary rheometer and calculated that the shear rate is 3.7 times the rotational speed.

Although correlations between the shear rate and the rotation speed in the Haake mixer have been developed by several researches, the application of the correlation for dispersive mixing

(droplet breakup) in the Haake blender is quite limited.⁴ Cheng and Manas-Zloczower¹⁵ have investigated the type of simple shear flow in the internal mixer such as the Banbury. According to Taylor's theory of drop breakup in simple shear flow,¹⁶ a minimum size of the dispersed drop is achieved when the viscous forces are equal to the interfacial tension. In order to predict the dispersive characteristics of a polymer mixture prepared in the Haake mixer, the effective shear rate needs to be considered.

In this study, a new simple mixing approach (without using torque data) is proposed to develop the correlations between the effective shear rate range for mixing and rotational speed in the Haake mixer. The effective shear rate range for mixing in the Haake mixer is determined by an analysis of flow in the mixer. Finally, the correlation relation-

Table I Characterization of Polymers

Polymer	M_n^a	Density (g/cm ³) ^a
LLDPE	69,800	0.924
PS	200,000	1.04
S-EP	45,000/115,000	0.91
S-EB-S	7,000/37,500/7,000	0.91

^a Provided by the suppliers.

ships were verified with mixing data (droplet size) generated during Haake blending.

A previous study¹⁷ has reported the morphology development during noncompatibilized and compatibilized polymer blending. In this work, the influences of processing parameters including mixing time, temperature (as it affects the viscosity ratio), composition, the rotor speed, and the type of compatibilizers on the blend morphology of polystyrene (PS) and linear low-density polyethylene (LLDPE) prepared in the Haake blender were investigated.

EXPERIMENTAL

Materials

The LLDPE used in this study is SCLAIR 2107, supplied by DuPont of Canada. The PS is Styron 680, obtained from the Dow Chemical Company. Styrene-ethylene/butylene-styrene (SEBS Kraton G1652) triblock, and styrene-ethylene/propylene (SEP Kraton G1702) diblock copolymers, supplied by the Shell Company, are used as the compatibilizers. Characterization of the polymers is listed in Table I.

Mixing

To study the shear rate correlations, blends of a low composition (2%) PS with LLDPE were prepared by mixing for 10 min in the Haake mixer. Three rotor speeds, 20, 50, and 100 rpm, were used. The melt temperature was set at 180°C.

Several blends of PS and LLDPE, under the different blending conditions, were prepared using the

Table III Haake Torque (g m) at 50 rpm vs. Temperature for Polymers

Temperature	LLDPE	PS	SEP	SEBS	η_{PS}/η_{LLDPE}
180°C	170	210	—	—	1.2
240°C	140	6 ^a	375	150	< 0.04

^a At 120 rpm.

Haake blender to study the processing-morphology relationships. The blending conditions investigated in this study are shown on Table II.

The viscosity ratio of PS to LLDPE as a function of temperature was determined by the ratio of the torque values for the pure components.^{12,18} At 50 rpm, the torque values and viscosity ratio of PS to LLDPE at 180 and 240°C are shown in Table III.

In addition, the dispersion behavior of the compatibilized blends with the styrene-ethylene/propylene (SEP) or styrene-ethylene/butylene-styrene (SEBS) block copolymer at a 5% level were studied under the various blending conditions and mixing sequences.

After 10 min of mixing in the Haake mixer, the blend samples were removed and solidified in liquid nitrogen to obtain fractured sample for the scanning electron microscope (SEM) examinations.

Characterization of Dispersive Morphology

Electron Microscopy

An (SEM), Jeol 5400, was used to examine the size and shape of the dispersed phase. The blend samples were fractured in liquid nitrogen, then used for SEM analysis. Details of the sample preparation procedure are discussed elsewhere.¹⁸

Image Analysis

The dispersed particle sizes were determined by means of semiautomated image analysis, developed in the University of Maryland-College Park (UMCP) Polymer Mixing Program. The SEM micrograph of the fractured sample was first scanned and converted into a digitized image. The digitized

Table II Blend Conditions Investigated

System	Composition	rpm	Temperature
PS/LLDPE	2/98, 5/95, 20/80, 30/70, 40/60	50, 100	180°C, 240°C

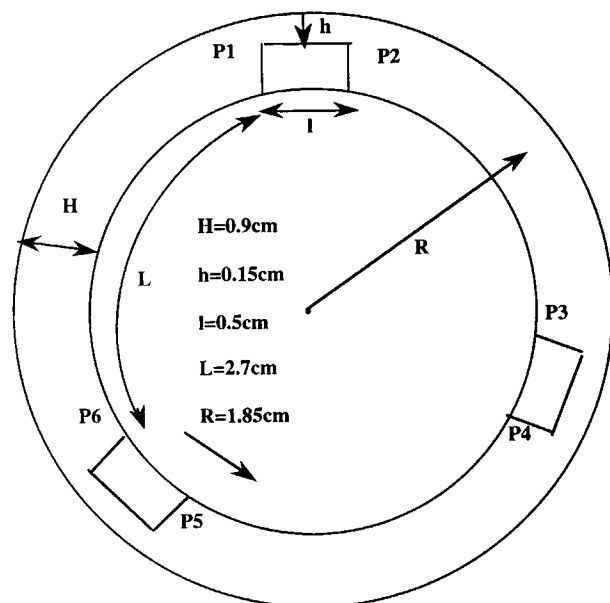


Figure 2 Schematic of a simplified Haake mixer. A modification of the Tadmor and Gogo model (1979).²¹

image is analyzed by a "Image 1.44" program to obtain the diameters of the dispersed particles.

The dispersion of PS in LLDPE is characterized through the number-average dispersed phase diameter d_n , the volume average diameter d_v (the moment mean diameter), and the size distribution curve. The values of d_n and d_v have been determined using 50–200 particles from three fields of view for each system. Increasing the number of measurements to 250 did not significantly alter the results.

It has been shown that the droplet is not monodispersed during breakup.¹⁹ When particles of many sizes occur together, a single parameter is inadequate to describe the sizes of all the particles that are present. A number of curve-fitting equations for particle size distribution have been proposed.²⁰ In this work, by examining particle size distribution during blending, there is not a general distribution function that can describe all the results, especially during the initial blending stage and in the compatibilized blends. We used the number-average particle diameter plus the standard deviation to give a range of particle size generating during polymer mixing. On the other hand, according to the manner in which the droplets deform and break up when sheared,¹⁹ each breakup event leads to a few very small satellite droplets between two daughter drops, for the range of viscosity ratio investigated in this study ($0.005 < \lambda < 3$). The volume average diameter, dominant by large particles, is close to the size determined from theory¹⁶ in which only two daughter drops are

produced after breakup. Other averages may alternatively be used without changing the qualitative features of our analysis.

RESULTS AND DISCUSSIONS

Shear Rate Correlations Based on Mixing Approach

Previous studies have successfully converted the Haake torque–rheometer data into fundamental rheological units. However, this type of correlations, based on what we called "the torque approach," uses the viscosity–temperature relationship and a rotational viscometer analogy to calibrate the shear rate with the rotor speed without the consideration of mixing. This study attempts to correlate the rotor speed with the shear rate in order to describe the mixing characteristic in the Haake blender. In addition, the computed shear rate value was compared to the literature value,⁴ 3.7N, which has been used as a basis for evaluation of the dispersed morphology.

Flow in a Banbury mixer has been modeled by Tadmor and Gogos,²¹ who considered it to be a highly simplified idealized internal mixer consisting of two infinitely long concentric cylinders with a short low clearance section. In this study, the same hydrodynamic analysis has been applied to a simplified Haake mixer geometry consisting of three gaps and three deep sections inside the concentric cylinders (see Fig. 2). The flow analysis and the shear rate calculations are detailed in Appendix A.

The shear rates in the Haake mixer calculated by different methods are shown in Table IV. Due to the complex geometry of the irregular rollers, we believed that there should be a distribution of shear rates prevailing at the roller surfaces. Therefore, in order to correlate the shear rate more precisely to the mixing process in the Haake mixer, an effective

Table IV Shear Rate in Haake Calculated by Different Methods

	In Gap	In the Deep Section
$\dot{\gamma}_{average}$	1.14N	0.29N
$\dot{\gamma}_{max}$	1.80N ($\dot{\gamma}_U$)	0.74N
$\dot{\gamma}_{drag\ flow}$	1.2N	0.22N ($\dot{\gamma}_L$)
$\dot{\gamma}_{literature} (\dot{\gamma}_s)$		3.7N

Table V Data Correlations for the Effective Shear Rate Range in a Haake Mixer

$\dot{\gamma}$ (s ⁻¹)	N = 20			N = 50			N = 100		
	$\dot{\gamma}_s = 74$	$\dot{\gamma}_U = 36$	$\dot{\gamma}_L = 4.4$	$\dot{\gamma}_s = 185$	$\dot{\gamma}_U = 90$	$\dot{\gamma}_L = 11$	$\dot{\gamma}_s = 370$	$\dot{\gamma}_U = 180$	$\dot{\gamma}_L = 22$
$\eta_{C-LLDPE}$ (Pa s)	1608	1881	3012	1312	1540	2457	1125	1320	2106
$\eta_{PS}/\eta_{LLDPE} = \lambda$	0.67	0.91	2.33	0.45	0.62	1.55	0.33	0.45	1.14
d_{Taylor} (μm) ^a	0.04	0.08	0.39	0.02	0.04	0.19	0.01	0.02	0.11
d_{Wu} (μm) ^a	0.27	0.36	3.56	0.19	0.25	1.24	0.14	0.19	0.56
$d_{n,exp}$ (μm)	1.26 (± 0.38)			0.94 (± 0.23)			0.63 (± 0.21)		
d_v (μm)	1.37			0.99			0.70		

$$^a d_{Taylor} = \sigma_{12}/\eta_c \dot{\gamma} [(16\lambda + 16)/(19\lambda + 16)], d_{Wu} = 4\lambda^{+0.84}(\sigma_{12}/\eta_c \dot{\gamma}) + \text{for } \eta > 1, - \text{for } \lambda < 1.$$

shear rate range for mixing was determined for the maximum ($\dot{\gamma}_U = 1.80N$) and minimum shear rates ($\dot{\gamma}_L = 0.22N$) based on the calculations.

We compared the experimentally determined particle size of the 2% PS dispersed phase with the predicted size values for different shear rates, based on Taylor's theory for a Newtonian droplet, as well as Wu's empirical model for viscoelastic polymer blends.⁷

Table V shows the correlations of the droplet size data with the different shear rates. The rheological properties of the blend materials were determined by the data provided by the companies (see Fig. 3). 5.8×10^{-3} N/m of the interfacial tension is taken from the literature.²² From the droplet size data, it seemed that $3.7N$, the shear rate for Haake mixers presented in the literature, is too high. On the other hand, based on Wu's equation for viscoelastic systems, the actual droplet sizes fell within the size range between the minimum shear rate and the maximum shear rate determined from our mixing approach. The shear rate of low-speed and high-speed viscometer, $0.76N$ and $1.14N$, calculated from the torque approach are included in the effective shear rate range from our calculations.

Processing–Morphology Relationships

Effect of Mixing Time

In the first part of this study,¹⁷ the morphological observations indicated that dispersion occurs at a very early stage of the polymer mixing process. A bimodal size distribution of the PS particles was observed during the initial stage of blending of 20% PS with 80% LLDPE, and of the same blend containing 5% of SEP or SEBS copolymers in the Haake blender. Figure 4 shows the effect of mixing time on the number-average domain size for the noncompatibilized and the compatibilized blends. It was found that for the noncompatibilized blend, the

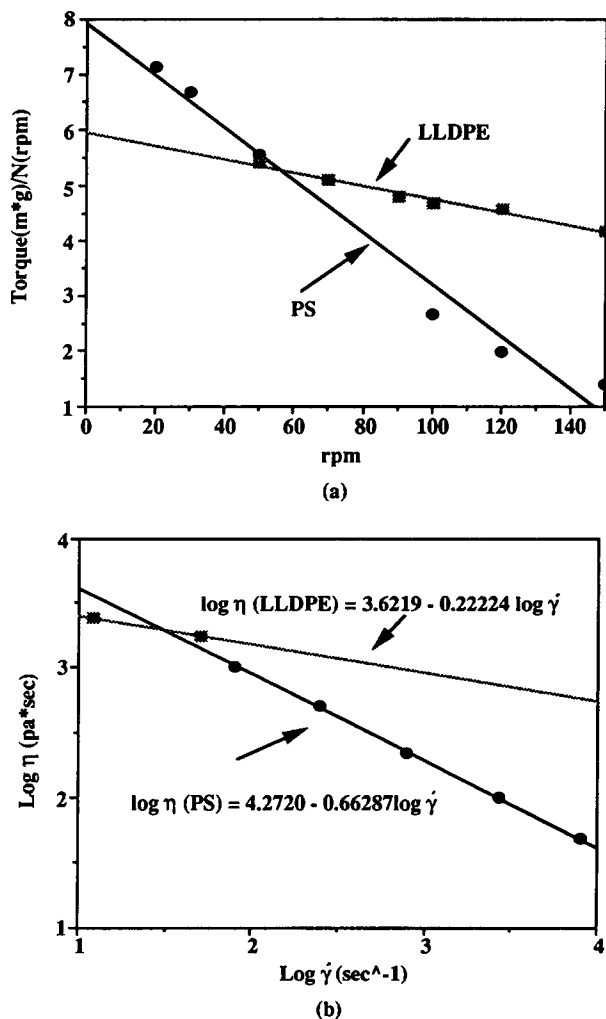


Figure 3 Rheological data for PS and LLDPE at 180°C: (a) measured in the Haake mixer and (b) obtained from companies.

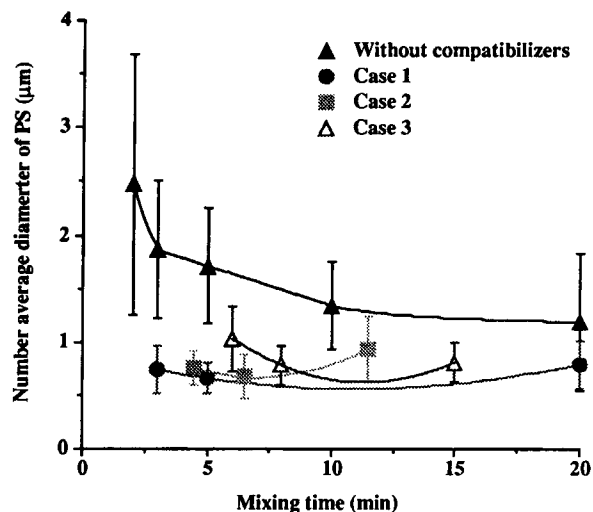


Figure 4 Effects of mixing time on the dispersed particle size (in groups of $2 \mu\text{m}$) at 180°C and 50 rpm. The standard deviations were indicated by error bars. (\blacktriangle) 20 PS/80 LLDPE, (\bullet) 19 PS/5 SEP/76 LLDPE. Case 1 when SEP was added at $T = 0$, case 2 when SEP was added at $T = 1.5$ min, case 3 when SEP was added at $T = 5$ min.

average domain size decreased as the mixing time increased. Further examining the size distribution (see Fig. 5) showed an increase in the number of the

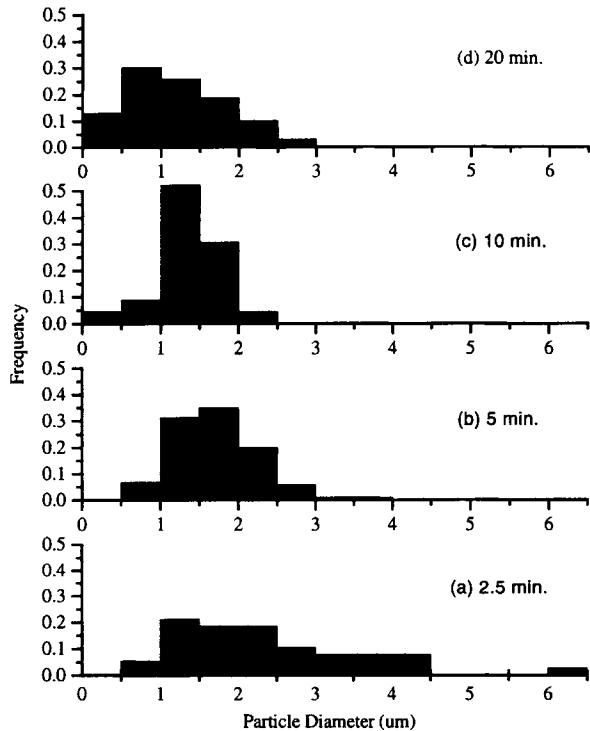


Figure 5 Effect of mixing time on the particle size distribution for the noncompatibilized blend of 20 PS and 80 LLDPE, 180°C and 50 rpm.

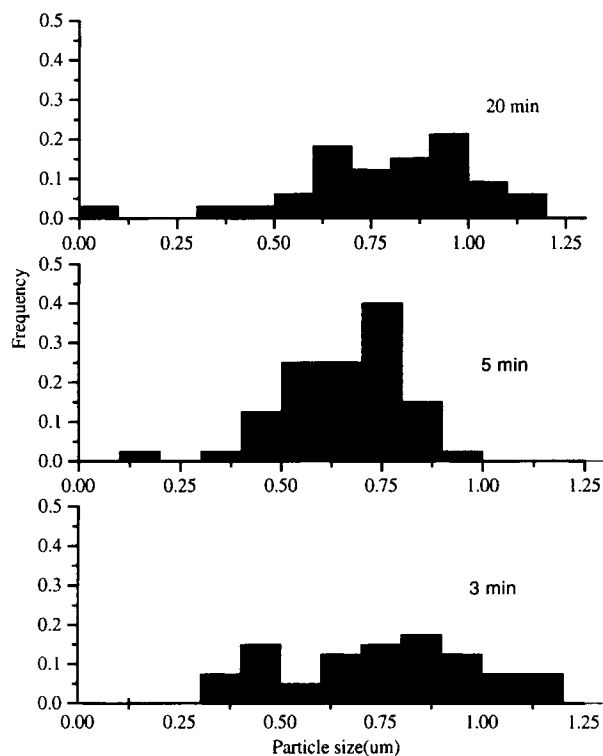


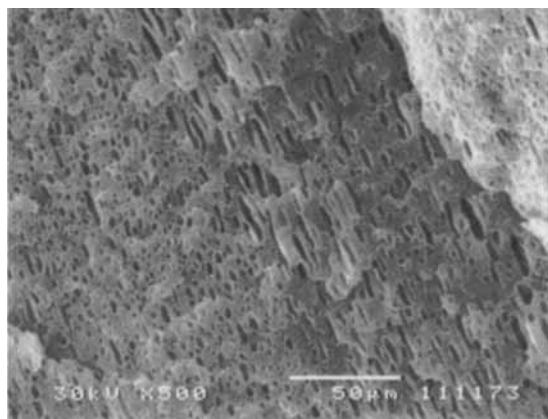
Figure 6 Effect of mixing time on the particle size distribution for the compatibilized blend of 19 PS/5 SEP/76 LLDPE (case 1), 180°C and 50 rpm.

larger particles in blends mixed from 10 to 20 min. For the 19 PS/5 SEP/76 LLDPE compatibilized blends, the domain size passed through a minimum with the mixing time for three different mixing sequences. A broader size distribution with an increased number of larger particles was observed in the end of the mixing process (see Fig. 6). This phenomena is supported by the work of Plochocki et al.,⁸ who found the minimum domain size when the mixing energy was increased. Their calculations indicated that the total interfacial energy in the polyblend and polyalloy is a trivial part of the mixing energy introduced.

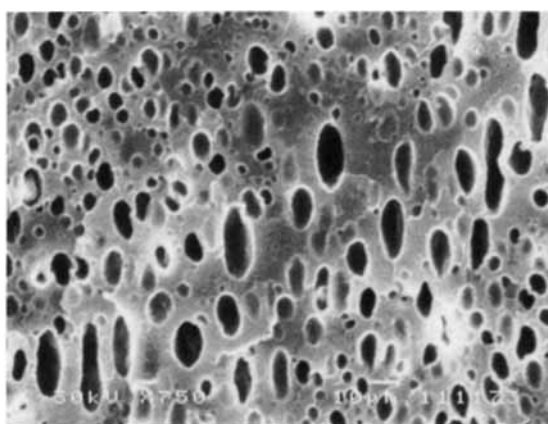
Effects of Composition and Blending Conditions

SEM photomicrographs showed that, at 180°C , where the viscosity ratio of PS and LLDPE is 1.2, the droplet type of dispersion of PS formed in the matrix of LLDPE for every composition investigated. As the temperature increased to 240°C , the viscosity ratio dropped to a value much less than 1 (< 0.04), which induced a fiber morphology of 30 and 40% PS in LLDPE (see Fig. 7).

Van Oene²³ argued that incompatible blend morphology is determined by the viscoelastic properties



(a)



(b)

Figure 7 SEM micrographs of blends of PS/LLDPE at 240°C, 50 rpm. (a) 30 PS/70 LLDPE and (b) 40 PS/60 LLDPE.

of the blend components. Specifically, the normal stress function as the interfacial tension is influenced by the elastic energy in the two phases. There is, however, no direct evidence of this argument shown in the other work, by Min and White.²⁴ They concluded that the differences in chemical composition and viscosity ratio are correlated with the coarseness of the phase morphology or with the droplet-fibril transitions for the blend systems. The greater the differences in polarity of the blend components, the greater the scale of phase dimensions. The experimental results presented in this study suggest that

the fiber morphologies result from lower viscosity and higher concentration of dispersion phases.

The influence of composition on the final average domain size for three blending conditions is shown in Figure 8. The experimental results indicate that, due to the balance of breakdown and coalescence of the droplets, the final dispersed phase size increased as the composition of PS increased. The data shown in Figure 8 indicates that the dispersed particles become larger for a given composition at 240°C when the viscosity ratio is far from unity. The influence of the viscosity ratio on the dispersed phase size was found to be a minor effect at a lower composition (20% PS) and to become more significant at the higher compositions of 30 and 40% PS. The finding that viscosity ratio has only an interactive effect was similarly found to be true in the case of blending miscible fluids.²⁵ This is in contrast to the observation of the influence of the shear intensity on the dispersed phase size. Increase of the rotor speed from 50 to 100 rpm had little effect on reducing the particle size in blends of 30 and 40% PS. The particle size distribution broadens with increasing the PS content. A much lower viscosity ratio than unity resulted in a broader size distribution.

The influence of the viscosity ratio on the deformation and breakup of droplets has been reported widely in the literature.^{16,26} Previous studies⁷ show that the dispersed drop size is at a minimum when the viscosity ratio is equal to 1. This is based on the assumption that there should be a maximum transfer of the stress across an interface when the viscosities of the two phases are equal. However, the recent study by Janssen et al.²⁷ reported that more realistic mixing is controlled by a transient mech-

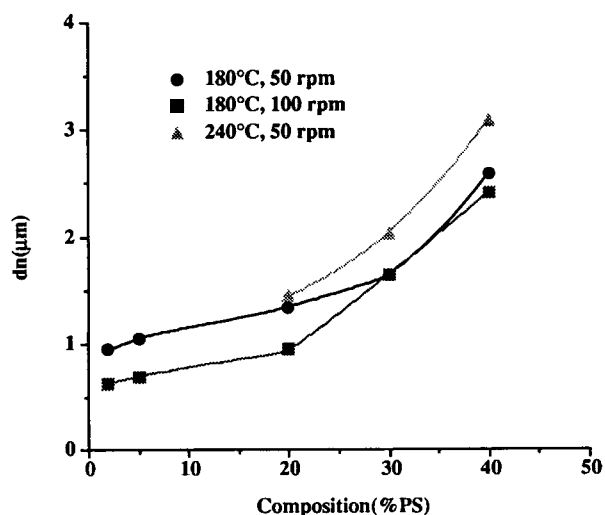


Figure 8 Effects of blending conditions on dispersion.

anism of thread breakup during extension (not by stepwise breakup under equilibrium conditions—Taylor's theory), which predicts that a viscosity ratio of unity is not optimum for obtaining the finest dispersion. Rather than that, a higher viscosity ratio between the dispersed and continuous phases yields a finer dispersion.

The above discussions explain the observed coarser PS particles, with a lower viscosity ratio, at 240°C. The manner in which the droplets elongate and break up when sheared is important, both theoretically and practically.²⁶ Looking at the manner of droplet breakup suggests that a wider size distribution due to the tip streaming mode of breakup might be obtained when the viscosity ratio is much less than 1, as compared with that in which the viscosity ratio is close to 1.

The effect of shear stress, as considered in Taylor's equation for Newtonian drops in a simple shear flow, indicates that the phase size is inversely proportional to the shear stress (or shear rate). Although large differences in shear stress clearly result in morphological changes, some authors²⁸ have indicated that varying the shear stress by a factor of 2–3 has little or no effect on the morphology. For polycarbonate/polypropylene (PC/PP) blends, Favis¹⁵ also concludes that above a critical shear stress blends are not sensitive either to shear stress or to shear rate. The results of this study are consistent with the previous work. Moreover, the results point out that the insensitivity of the dispersed phase size to the shear intensity is more apparent at higher concentrations of the minor phase. A possible explanation for the high insensitivity may be that shear stress and shear rate are not continuous at the interface of the immiscible binary blend. The poor stress transfer across the boundary phase may be the cause of these unexpected deviations from Taylor's theory.

For blends of 20% PS and 80% LLDPE at 180°C, a step change of rotor speed (shear rate) was introduced to investigate transient effects during mixing in the Haake mixer. The experiment was run in such a way that rotor speed was increased from 20 to 50 rpm in steps of 10 rpm. Each of the step changes lasted 1 min. After each incremental increase in speed, the machine was stopped for 10 s, and the machine started again at the new increased speed. The total mixing time was 4.5 min. A steady-speed-increase experiment was run in the same way without stopping of the machine ($\Delta N/\Delta t = 10$ rpm/min). The results showed that there is no significant effect of the rate of change in shear rate on the final domain size ($d_{n,transition} = 1.57 (\pm 0.69) \mu\text{m}$, and $d_{n,steady} = 1.53 (\pm 0.68) \mu\text{m}$) and the size distribution. It

seemed that the results did not support the previous study by Flumerfelt,⁶ who suggested that the transient flow was preferable for dispersion in viscoelastic systems. One possibility might be that the irregular-shaped rollers in a Haake mixer provide the transient flow which controls the dispersion.

Combined Effects of Blending Conditions and the Compatibilizers

Table VI shows the combined effects of blending conditions and the compatibilizer on the dispersed phase size of PS/LLDPE blends. The results show the superiority of the triblock SEBS over the diblock SEP, in reducing the dispersed phase dimensions for different blending conditions and compositions. The higher emulsifying efficiency of the SEBS copolymer on the dispersion is even more evident at higher amount of the dispersed phase.

It is concluded that, contrary to what was expected from theory, the shear intensity (rpm) did not significantly improve the final dispersion in the immiscible binary blend. The addition of the compatibilizer changed the interfacial conditions between the two immiscible phases and reduced the critical shear stress for breakup. By adding the compatibilizer, the adhesion at the PS/LLDPE boundary allowed good stress transfer across the interface. Therefore, when the roller speed of the Haake mixer was doubled, there was a pronounced reduction in

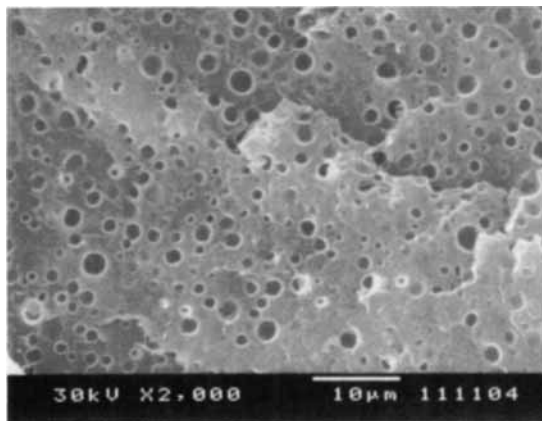
Table VI Dispersed Phase Dimensions (μm) of PS/LLDPE Blends with the Compatibilizer at 5% Level

Blending Conditions	Compatibilizer	Composition	
		20/80	40/60
180°C, 50 rpm	—	1.34 (± 0.41)	2.59 (± 1.13)
	SEP	0.79 (± 0.23)	1.77 (± 0.73)
	SEBS	0.64 (± 0.14)	0.83 (± 0.33)
180°C, 100 rpm	—		2.41 (± 1.24)
	SEP		1.26 (± 0.52)
240°C, 50 rpm	—	1.44 (± 0.63)	3.08 (± 1.35)
	SEP	1.11 (± 0.40)	2.67 (± 0.86)
	SEBS	0.64 (± 0.14)	0.73 (± 0.26)

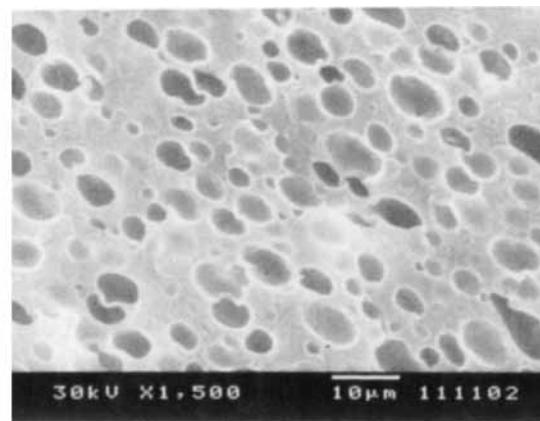
particle size of the dispersed phase from 1.77 to 1.26 μm for the 38 PS/5 SEP/57 LLDPE blend. Compared with the binary system, the reduction rate of the dispersed phase dimensions was 7% in 40 PS/60 LLDPE and 29% in 38 PS/5 SEP/57 LLDPE, during a twofold increase of the roller speed.

At 240°C and 50 rpm, the addition of SEP diblock copolymer did not significantly reduce the dispersed phase dimensions of the PS/LLDPE blends (Fig. 9). This result raised the question whether or not SEP accumulates at the interface between PS and

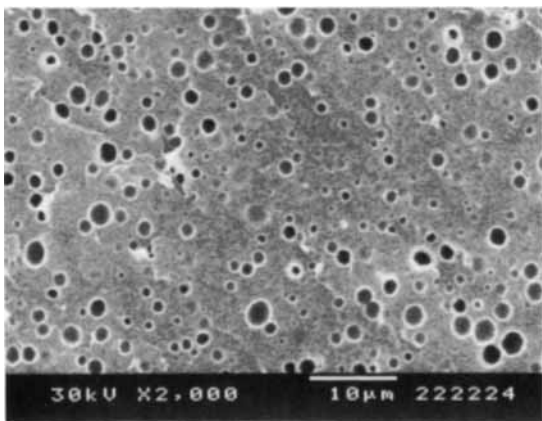
LLDPE. Experimental results from dynamic mechanical measurements have shown the improved adhesion between the phases of LLDPE and PS upon the addition of SEP,¹⁸ which indicates the existence of SEP at the interface. The microphase separation in SEP, thought to be associated with the resulting morphology instability, no longer exists at a higher temperature (where χN_p is so small that the copolymer melt would exhibit a homogeneous disorder phase, χ is interaction parameter, N_p is polymerization index), and therefore there is no pen-



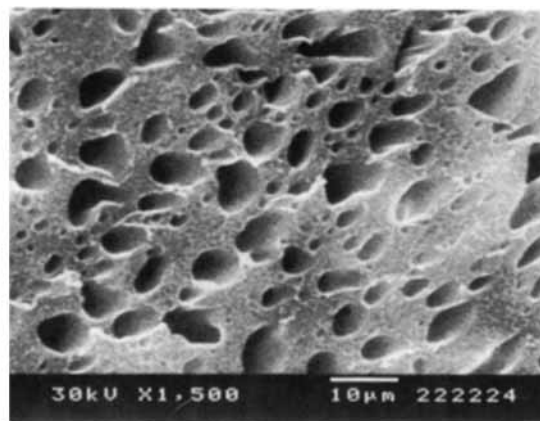
(a)



(c)



(b)



(d)

Figure 9 SEM micrographs of blends of PS/LLDPE at 240°C, 50 rpm: (a) 20 PS/80 LLDPE, (b) 19 PS/5 SEP/76 LLDPE, (c) 40 PS/60 LLDPE and (d) 38 PS/5 SEP/57 LLDPE.

etration of segments in the respective homopolymer phase.²⁹ On the other hand, the addition of the triblock SEBS into the blend not only reduced but also stabilizes the sizes of the dispersed particles so that the final dispersed dimensions become independent of the compositions.

In this study, a 5% level of the compatibilizers was arbitrarily chosen. Previous studies^{11,30} demonstrated that the addition of a small amount of the copolymer significantly improve both the dispersion and the strength properties of the immiscible polymer blends. Therefore, it is of interest to determine the minimum quantity of SEP and SEBS copolymers required to achieve the same dispersion as obtained in this study when 5% copolymers were added.

In making these calculations, several assumptions were made. First, the interface between PS and LLDPE phases are saturated by the block copolymers. The interfacial area occupied by each copolymer chain (S/n_c), being a function of the molecular weight, is determined by the experimental data presented by Hashimoto et al.³¹ for polystyrene/polyisoprene copolymers of the same molecular weights of the SEP and SEBS copolymers. The volume fraction of SEP is calculated to be 4.3% (see Appendix B) and can be converted to the weight fraction of 4%. For 19 PS/5 SEBS/76 LLDPE, $MW = 51,500$ and $S/n_c = 7 \text{ nm}^2$,³¹ the required amount of 2 wt % SEBS was calculated for the saturation of the interface with the PS particles of $0.65 \mu\text{m}$.

The above results indicates that a 5 wt % level of the copolymer concentration is a reasonable value to show the emulsification efficiency of adding the copolymer to the blends. Furthermore, in order to achieve the same degree of dispersion (the same particle size in 20 PS/80 LLDPE system) in blends of 40 PS and 60 LLDPE, the required percentage of SEP and SEBS was calculated to be about 7.5 and 4 wt %, respectively. To validate the theoretical calculations, 2.5% SEBS and 7.5% SEP were mixed with blends of a 20 PS/80 LLDPE ratio and a 40 PS/60 LLDPE ratio, respectively, for 10 min at 180°C and 50 rpm. The blend morphology of 19.5% PS/2.5% SEBS/78% LLDPE in Figure 10 showed that some PS particles are about the same size as those in the noncompatibilized blends, which indicated that an amount in excess of 2.5% is required for saturation of all the PS particles. On the other hand, no significant reduction of the PS phase scale was observed when 7.5% SEP was added to 37% PS/55.5% LLDPE blends. Similar observations were reported by Lim and White,⁹ who found that a great excess of MASEBS (functionalized SEBS with maleic anhydride) (5%) than required (0.5%)

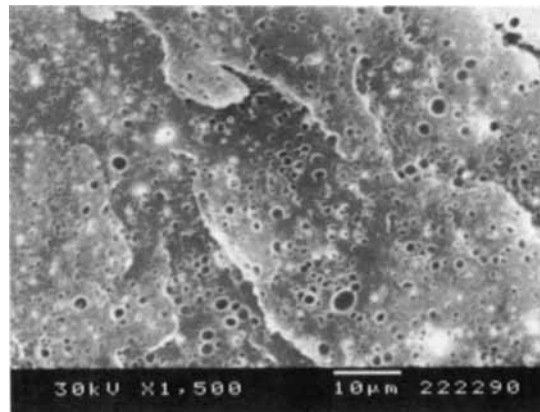


Figure 10 SEM micrographs of blends of 19.5 PS/2.5 SEBS/78 LLDPE.

is needed for the successful compatibilization of a 75% polyethylene/25% polyamide-6 blend prepared in a co-rotating twin-screw extruder. It seems that a higher concentration of the copolymer improves the probability that the copolymer can reach the interface. Transport of the copolymer to the interface may be hindered by the high viscosity of the melt.

CONCLUSIONS

A new simple mixing approach for the correlations of the effective shear rate range for dispersive mixing in the Haake mixer is proposed based on a flow analysis of a simplified internal mixer. The effective shear rate range was determined to range from $0.22N$, the shear rate in the deep section without considering the pressure flow, to $1.80N$, the maximum shear rate in the gap. The experiment results suggest that $3.7N$, the shear rate for the Haake mixer presented in the literature, is too high to fit the experimentally determined droplet size of a 2% PS blend with LLDPE at 180°C .

The mode of dispersion was determined by the composition and the rheology of the mixture. The fiber/stratified morphologies form with blends that contain the minor phase of a lower viscosity and at high concentration. The final dispersed phase size increases as the composition of PS increases. Coarse dispersed particles are obtained in blends having viscosity ratios far from unity. The influence of the viscosity ratio on the dispersed phase size is found

to be a minor effect at a lower composition (20% PS). Doubling the rotor speed had little effect on reducing the particle size of 30 and 40% PS blends. The size of PS particles broadens with increasing weight fraction of PS. A much lower viscosity ratio than unity results in a broader size distribution.

Both SEP and SEBS are good compatibilizers for blends of PS with LLDPE at 180°C. The superiority of the triblock SEBS over the diblock SEP copolymer in reducing the dispersed phase dimensions is shown for different blending conditions and compositions. At 240°C, the addition of SEP did not apparently improve the degree of dispersion. On the other hand, the addition of SEBS into the blend stabilizes the dispersed phase without coalescence so that the final dispersed dimensions became independent of the compositions. Adding the compatibilizer increased the adhesion at PS/LLDPE boundary and allowed a good stress transfer across the interface. The effect of shear stress on phase size, therefore, is more pronounced in the compatibilized blend.

The theoretical amounts of the copolymers required for saturation of the interface between two immiscible phases were calculated. A 5% level of the compatibilizers is indicated as a reasonable value to demonstrate emulsification. Due to a dynamic mixing process in the Haake mixer, an larger amount than that calculated of the compatibilizers is needed for saturation of all the PS droplets.

APPENDIX A

From Figure 2, if the curvature is neglected ($H/R \ll 1$), the flow can be considered as parallel-plate flows in rectangular coordinates. The flow takes place between an infinite upper plate moving at constant velocity over a lower plate, with a step change in the clearance between them. Assuming the familiar simplified assumptions of laminar isothermal, incompressible steady Newtonian flow, no slip at the walls, negligible entrance and exit effects at the step, and neglecting gravitational forces leads to expressions for the flow rate, which is the same in the gap and in the deep section, in terms of local conditions.

$$\begin{aligned} q &= \frac{V_0 H}{2} - \frac{H^3 (P_1 - P_6)}{12 \mu_L L} = \frac{V_0 h}{2} - \frac{h^3 (P_2 - P_1)}{12 \mu_l} \\ &= \frac{V_0 H}{2} - \frac{H^3 (P_3 - P_2)}{12 \mu_L L} = \frac{V_0 h}{2} - \frac{h^3 (P_4 - P_3)}{12 \mu_l} \\ &= \frac{V_0 H}{2} - \frac{H^3 (P_5 - P_4)}{12 \mu_L L} = \frac{V_0 h}{2} - \frac{h^3 (P_6 - P_5)}{12 \mu_l} \end{aligned} \quad (1)$$

where $V_0 = \pi ND$, N is the shaft speed, D is the diameter of the roller; μ_l and μ_L are the fluid viscosities in the two regions, accounting approximately for the non-Newtonian melt behavior. However, in this work, by looking at the rheological properties of PE (see Fig. 3), it seems that the viscosities of PE were not very sensitive to the shear rate within the range mostly investigated. With this in mind, the equations are simplified so that the two regions are assumed to have the same viscosities.

Assuming the geometrical symmetry of the Haake mixer, only one third is treated. Rearranging Eq. (1), we obtain for the pressure drop over the "step"

$$\begin{aligned} \frac{\Delta P}{l} &= \frac{6\mu_l V_0}{h^2} K, \\ (\Delta P = P_1 - P_2 = P_3 - P_4 = P_5 - P_6) \\ K &= \frac{(H/h) - 1}{(H/h)^3 (l/L) (\mu_l/\mu_L) + 1} \end{aligned} \quad (2)$$

The velocity profile between two parallel plates were obtained as²¹

$$\frac{v_z}{V_0} = (y/h) + 3(y/h)[1 - (y/h)]K \quad (3)$$

By taking the first derivative of Eq. (3) with respect to y , we obtain:

I. In the gap

$$\dot{\gamma}\left(\frac{y}{h}\right) = \frac{V_0}{h} \left\{ 1 + 3K \left[1 - 2\left(\frac{y}{h}\right) \right] \right\} \quad (4)$$

The velocity weighted average shear rate is defined as

$$\begin{aligned} \dot{\gamma}_{\text{average}} &= \frac{\int_0^h |\dot{\gamma}_{yz}| V_z dy}{\int_0^h V_z dy} \\ &= \begin{cases} \frac{V_0}{h(1+K)}, & -\frac{1}{3} \leq K \leq \frac{1}{3} \\ \frac{V_0}{h} \left(\frac{1+3K}{6K} \right)^2 \frac{1}{1+K} \\ \quad \times \left[\frac{(1+3K)^2}{2} - 1 \right], & K \geq \frac{1}{3} \end{cases} \end{aligned} \quad (5)$$

The maximum shear rate at mixer wall is

$$\dot{\gamma}_{\max}|_{\text{at wall}} = \frac{V_0}{h} (1 + 3K) \quad (6)$$

The shear rate for drag flow only is expressed as

$$\dot{\gamma}_{\text{drag flow}} = \frac{V_0}{h} \quad (7)$$

II. In the deep section

The same equations hold with μ_l/h replaced by μ_L/H and K replaced by K' , which is defined as follows:

$$K' = \frac{1 - (h/H)}{(h/H)^3(L/l)(\mu_l/\mu_L) + 1} \quad (8)$$

For the dimensions of the Haake mixer (see Fig. 2) Eqs. (2) and (8) yield

$$\begin{aligned} K &= 0.13 \\ K' &= 0.81 \end{aligned} \quad (9)$$

APPENDIX B

The following calculations apply to blends of 19 PS/5 SEP/76 LLDPE: Assume total volume of the blend is $10^6 \mu\text{m}^3$. The droplet diameter of PS is $0.8 \mu\text{m}$. The volume fraction of PS in blends is

$$\begin{aligned} \varphi_{\text{PS}} &= \frac{19/1.04 + (5 \times 0.28)/1.04}{5/0.91 + 19/1.04 + 76/0.924} \\ &= 18.5\% \end{aligned} \quad (10)$$

The total surface area of PS particles is

$$\begin{aligned} \text{Total interface} &= \frac{0.185 \times 10^6}{4/3 \pi (0.8/2)^3} 4\pi (0.8/2)^2 \\ &= 13.88 \times 10^5 \mu\text{m}^2 \end{aligned} \quad (11)$$

For SEP, $\text{MW} = 160,000$, $S/n_c = 9.5 \text{ nm}^2$.²⁹ The total copolymer chains to fulfill the interface then is calculated as

$$\begin{aligned} N_c &= \frac{\text{total interface}}{\text{area per chain}} = \frac{13.88 \times 10^5 \mu\text{m}^2}{9.5 \text{ nm}^2} \\ &= 1.46 \times 10^{11} \end{aligned} \quad (12)$$

$\rho_{\text{SEP}} = 0.91 \text{ g/cm}^3$. The total volume of the SEP copolymer is

$$\begin{aligned} V_{\text{SEP}} &= \frac{1.46 \times 10^{11} \times 160,000}{6.02 \times 10^{23} \times 0.91} 10^{12} \mu\text{m}^3 \\ &= 4.3 \times 10^4 \mu\text{m}^3 \end{aligned} \quad (13)$$

NOMENCLATURE

$\dot{\gamma}$	Shear rate (s^{-1})
η	Melt viscosity (Pa s)
N	Rotational speed (rpm)
d	Droplet diameter (μm)
λ	Viscosity ratio
σ_{12}	Interfacial tension (N/m)
χ	Interaction parameter
N_p	Polymerization index
S	Interfacial area (nm^2)
MW	Molecular weight
ΔN	Speed difference (s^{-1})
q	Volume flow rate (cm^3/s)
n_c	Number of copolymer chains
ϕ	Volume fraction

The authors would like to express their appreciation to Drs. Briber and Pourdeyehemi for valuable discussions and to C. D. Merritt and I. S. Sei for aid in performing the mixing experiments. Special thanks are extended to GE Plastics, Dow Chemical, BF Goodrich, and Welding Engineers, members of the Polymer Mixing Program, for financial support and constructive advise during this work. Acknowledgment is also made to DuPont of Canada, Dow Chemical Co., and Shell Chemical Co. for supplying materials.

REFERENCES

1. J. M. Willis, B. D. Favis, and J. Lunt, *Polym. Eng. Sci.*, **30**, 1073 (1990).
2. S. Wu, *Polymer*, **26**, 1855 (1985).
3. S. Hobb, *Polym. Eng. Sci.*, **26**, 74 (1986).
4. G. Serpe, J. Jarrin, and F. Dawans, *Polym. Eng. Sci.*, **30**(9), 553 (1990).
5. B. D. Favis, *J. Appl. Polym. Sci.*, **39**, 285 (1990).
6. R. W. Flumerfelt, *Ind. Eng. Chem. Fundam.*, **11**(3), 312 (1972).
7. S. Wu, *Polym. Eng. Sci.*, **27**(5), 335 (1987).
8. A. P. Plochocki, S. S. Dagli, and R. D. Andrews, *Polym. Eng. Sci.*, **30**(12), 741 (1990).
9. S. Lim and J. L. White, *Polym. Eng. Sci.*, **34**(3), 221 (1994).
10. B. D. Favis and J. P. Chalifoux, *Polymer*, **29**, 1761 (1988).
11. R. Fayt, R. Jerome, and Ph. Teyssie, *J. Polym. Sci. Part B: Phys. Ed.* **27**, 775 (1989).

12. J. E. Goodrich and R. S. Porter, *Polym. Eng. Sci.*, **7**, 45 (1967).
13. L. L. Blyler, Jr., and J. H. Daane, *Polym. Eng. Sci.*, **7**, 178 (1967).
14. G. C. N. Lee and J. R. Purdon, *Polym. Eng. Sci.*, **9**(5), 360 (1969).
15. J. J. Cheng and I. Manas-Zloczower, *Polym. Eng. Sci.*, **29**(15), 1059 (1989).
16. G. I. Taylor, *Proc. Roy. Soc. (London)*, **146A**, 501 (1934).
17. L. Y. Yang, T. G. Smith, and D. Bigio, *J. Appl. Polym. Sci.*, to appear.
18. L. Y. Yang, Ph.D. Dissertation, Univ. of Maryland at College Park (1994).
19. H. J. Karam and J. C. Bellinger, *Ind. Eng. Chem., Fundam.*, **7**, 576 (1968).
20. L. Silverman, C. E. Billings, and M. W. First, *Particle Size Analysis in Industrial Hygiene*, Academic Press, New York, 1971, Chap. 6.
21. Z. Tadmor and C. G. Gogos, *Principles of Polymer Processing*, Wiley-Interscience, New York, 1979, Chapters 10 and 11.
22. C. C. Chen and J. L. White, SPE Antec. Papers, 1991, p. 969.
23. H. Van Oene, *J. Colloid. Interface Sci.*, **40**, 448 (1972).
24. Kyonsuku Min and James L. White, *Polym. Eng. Sci.*, **24**(17), 1327 (1984).
25. W. Baim, M.S. Thesis, University of Maryland at College Park (1994).
26. F. D. Rumscheidt and S. G. Mason, *J. Colloid. Sci.*, **16**, 238 (1961).
27. J. M. H. Janssen and H. E. H. Meijer, *J. Rheol.*, **37**(4), 597 (1993).
28. Z. K. Walczak, *J. Appl. Polym. Sci.*, **17**, 169 (1973).
29. L. Leibler, *Macromolecules*, **13**, 1602 (1980).
30. D. Heikens, N. Hoen, W. M. Barentsen, P. Piet, and H. Landan, *J. Polym. Sci., Polym. Symp.*, **62**, 309 (1978).
31. T. Hashimoto, M. Fujimura, and H. Kawai, *Macromolecules*, **13**, 1669 (1980).
32. Manufacturer, Haake Instruments, Inc., Paramus, New Jersey.

Received November 21, 1994

Accepted March 31, 1995